PHREEQ-N-AMDTreat+REYs Water-Quality Modeling Tools to Evaluate Acid Mine Drainage Treatment Strategies for Recovery of Rare-Earth Elements

C. A. Cravotta III

U.S. Geological Survey, Pennsylvania Water Science Center
215 Limekiln Rd., New Cumberland, PA 17070, USA cravotta@usgs.gov

ABSTRACT

The PHREEQ-N-AMDTreat+REYs water-quality modeling tools have the fundamental capability to simulate aqueous chemical reactions and predict the formation of metal-rich solids during the treatment of acid mine drainage (AMD). These new user-friendly, publicly available tools were expanded from the PHREEQ-N-AMDTreat tools to include the precipitation of rare-earth elements plus yttrium (REYs) and the adsorption of REYs onto hydrous Fe, Al, and Mn oxides. The tool set consists of a caustic titration model that indicates equilibrium surface and aqueous speciation of REYs as functions of pH and caustic agent, and a kinetics+adsorption model that simulates progressive changes in pH, major ions, and REYs in water and solids during sequential steps through passive and/or active treatment. Each model has a user interface (UI) that facilitates the input of water-quality data and adjustment to geochemical or treatment system variables; for example, retention time and aeration rate are adjustable parameters in the kinetics model. On-screen graphs display results of changes in metals and associated solute concentrations as functions of pH or retention time; details are summarized in output tables. A goal of such modeling is to identify strategies that could produce a concentrated REYs extract from AMD or mine waste leachate. For example, if REYs could be concentrated after first removing substantial Fe and Al, the final REYs-bearing phase(s) could be more efficiently processed for REYs recovery and, therefore, may represent a more valuable commodity. Preliminary modeling supports the hypothesis that Fe and Al can be removed at pH < 5.5 using conventional sequential oxidation and neutralization treatment processes without removing REYs, and that further increasing pH can promote the adsorption of REYs by hydrous Mn oxides. Alternatively, chemicals such as oxalate or phosphate may be added to precipitate REYs compounds following initial steps to decrease Fe and Al concentrations. The aqueous geochemical model framework is comprehensive and permits evaluation of effects from interactive chemical and physical variables. Field studies that demonstrate REYs attenuation from AMD and corresponding solid-phase formation during specific treatment steps plus laboratory studies of aqueous/solid interactions are helpful to corroborate, refine, and constrain modeling parameters.

Keywords: resource recovery, adsorption, precipitation, equilibrium, kinetics

1.0   INTRODUCTION

Many studies have reported elevated concentrations of rare-earth elements plus yttrium (REYs) plus other critical metals in acid mine drainage (AMD) and in associated solids formed during treatment to remove contaminants from the water (Cravotta, 2008; Vass et al., 2019a, 2019b; Hedin et al., 2020). For example, coal refuse (non-coal material removed during coal cleaning) frequently is pyritic and, consequently, the refuse leachate tends to be acidic and have some of the highest concentrations of REYs and associated metals compared to other types of AMD from coal mines (Cravotta and Brady, 2015). Management of the acidic, metal-laden leachate and solid

waste from coal refuse-disposal facilities is a long-term liability that will persist long after coal mines have closed. An economically sustainable approach for recovery of REYs from such leachate could offset treatment costs.

Routine treatment methods for acid neutralization and metals removal plus various additional steps may be applicable for the recovery of REYs from AMD. Various studies have investigated specific AMD treatment strategies and mechanisms for concentrating REYs by adsorption and/or precipitation with hydroxide, phosphate, or oxalate compounds (Ayora et al., 2018; Zhang and Honaker, 2018; Josso et al., 2018; Edahbi et al., 2018; Royer-Lavallée et al., 2020; Wang et al., 2021; Leon et al., 2021; Mwewa et al., 2022; Hermassi et al., 2022). Appropriate treatment and resource-recovery strategies must also consider the water quality, its volume, and location, plus environmental and economic factors (Fritz et al., 2021). If REYs could be concentrated after first removing substantial Fe and Al, which typically constitute a major fraction of treatment sludge, the final REYs-bearing phase(s) may be more concentrated in a smaller volume of solids formed at later steps. Solids having concentrated REYs may represent a more valuable commodity that can be efficiently transported and processed for REYs recovery, particularly if REYs can be extracted without total digestion of the solids.

Geochemical modeling coupled with cost-analysis software, such as AMDTreat (Office of Surface Mining Reclamation and Enforcement, 2017), may be applied to identify and evaluate treatment strategies for the potential range of variations in influent water quality and to compare costs for construction and operation of different treatment methods that produce the desired effluent quality. The PHREEQ-N-AMDTreat+REYs water-quality modeling tools described in this paper simulate changes in the pH and concentrations of REYs, Fe, Al, Mn, SO_4, and other solutes plus the formation of solids containing REYs in response to changing solution composition, the composition and availability of hydrous-metal-oxide (HMeO) sorbent, and the potential for REYs compounds and other solids to precipitate.

2.0   METHODOLOGY

The PHREEQ-N-AMDTreat+REYs tool set, which is available as a U.S. Geological Survey (USGS) software release (Cravotta, 2022), consists of a caustic titration model that indicates equilibrium aqueous and surface speciation of REYs and other elements as functions of pH and caustic agent, and a kinetics+adsorption model that simulates progressive changes in pH and element concentrations during sequential reaction steps through passive and/or active treatment. The PHREEQ-N-AMDTreat+REYs models were developed with the USGS aqueous speciation program PHREEQC (Parkhurst and Appelo, 2013) and complement the PHREEQ-N-AMDTreat tools (Cravotta, 2020, 2021), which do not consider REYs, other trace elements, fluoride, phosphate, or oxalate. Unlike direct PHREEQC coding, which requires input of values for the solution composition and other model variables, the PHREEQ-N-AMDTreat tools employ a user interface (UI) that facilitates input of initial solute concentrations and adjustment to system variables, such as the potential for precipitation of minerals and/or the availability and properties of HMeO sorbent, without changing the underlying PHREEQC coding. The tools permit mixing of two input solutions, A and B, prior to reactions based on user-specified mixing ratios or flow rates of A and B to compute the volume-weighted concentrations in a 1-L solution, which is the fundamental unit in PHREEQC. The new models utilize the wateq4fREYsKinetics.dat thermodynamics plus kinetics database, which was expanded from wateq4f.dat (Ball and Nordstrom, 1991) provided with PHREEQC to include REYs aqueous and surface species plus

relevant REYs solid phases (hydroxide, carbonate, phosphate, and oxalate compounds). Surface species for REYs plus other cations and anions are considered for hydrous ferric oxide (HFO: Dzombak and Morel, 1990; Verplanck et al., 2004; Liu et al., 2017), hydrous aluminum oxide (HAO: Karamilidis and Dzombak, 2010; Lozano et al., 2019), and hydrous manganese oxide (HMO: Tonkin et al., 2004; Pourret and Davranche, 2013), which together constitute the total HMeO sorbent capacity. Sources of data and values for selected thermodynamic or rate constants are summarized in the software release (Cravotta, 2022). The rate models included in wateq4fREYsKinetics.dat are identical to those in phreeqcAMDTreat.dat previously described by Cravotta (2020, 2021).

The diffuse double layer model of Dzombak and Morel (1990), with an inner surface layer and an outer diffuse layer of counter ions in solution, is used to simulate surface complexation by the HMeO sorbents. Adsorption is computed for freshly precipitated HFO, HAO, and/or HMO plus previously accumulated HMeO that has a specified constant mass and composition. The latter may occur as suspended or recirculated solids or coatings on treatment media. Multiple phases that may precipitate upon reaching equilibrium are considered for the fresh HMeO sorbent: HFO is amorphous $Fe(OH)_3$ plus $Fe(OH)_2$; HAO is amorphous $Al(OH)_3$ plus basaluminite ($Al_4(OH)_{10}SO_4$); and HMO is $Mn(OH)_3$ with solubility of manganite plus $Mn(OH)_2$. Each of the HFO, HAO, and HMO sorbents is considered to have uniform sorbing characteristics indicated by the specific surface area (Asp), site density (n), and surface-binding constants for cations and anions. Based on various literature sources reported by Cravotta (2021, 2022), default values for sorbents and other system parameters are provided automatically in the initial input file. The default Asp and n for each of the sorbents (HFO 600 m^2 g^{-1} and 1.925 sites nm^{-2}; HAO 68 m^2 g^{-1} and 4.6 sites nm^{-2}; HMO 746 m^2 g^{-1} and 1.91 sites nm^{-2}), which may be adjusted in the UI, determine the moles of strong (inner layer) and weak (outer layer) sorption sites with each mole of HFO, HAO, and HMO.

In addition to the precipitation of various Fe, Al, and Mn solids, which may form fresh sorbent, the model also simulates the potential for precipitation of REY-hydroxide, carbonate, phosphate, or oxalate compounds. In general, adsorption and precipitation processes compete with one another. Possible effects from precipitation of REYs and other solids can be evaluated by adjusting the saturation index (SI) value for selected compound(s), as explained by Cravotta (2021). Changing the SI (from the value 0 for equilibrium) is equivalent to changing the equilibrium constant for the precipitation-dissolution reaction. Precipitation of a less soluble phase is simulated by decreasing SI, whereas a relatively soluble phase is simulated by increasing SI. In the extreme case, selecting the SI value of 99 prevents precipitation of the solid. Thus, if one wishes to simulate sorption by HAO consisting of only $Al(OH)_3$, the SI value for basaluminite would be set to 99 and that for $Al(OH)_3$ would be set to 0 (or another value near 0).

Corresponding changes in the equilibrium distribution of REYs and other solutes between aqueous, sorbed, and precipitated fractions are indicated by on-screen graphs and selected output files. Output includes the concentrations of REYs and other solutes in effluent and the accumulated mass of REYs in solids from the combined total REYs adsorbed and precipitated.

2.1 Caustic titration equilibrium-adsorption-precipitation model

The CausticTitrationMix2REYsMoles.exe and CausticTitrationMix2REYs.exe tools consider REYs attenuation from solution by adsorption to HMeO (fresh and/or previously formed) and/or

by precipitation as solid compounds (Cravotta, 2022). The aqueous and surface speciation reactions are simulated as equilibrium processes that respond to instantaneous changes in pH and sorbent availability. The pH is increased by 0.25-unit intervals from the initial pH value to a maximum value of 11 by the addition of a selected acid-neutralizing (caustic) agent (NaOH, $Ca(OH)_2$, CaO, Na_2CO_3, or $CaCO_3$). Cravotta et al. (2015) and Cravotta (2021) provided background on AMD neutralization by these caustic agents and offered additional tools for computing estimated caustic quantities to achieve pH targets for "raw" unaerated or aerated AMD.

2.2   Sequential kinetics-adsorption-precipitation model

The TreatTrainMix2REYs.exe tool simulates sequential steps in a passive and/or active AMD treatment system (Cravotta, 2022). Kinetics processes such as CO_2 outgassing, O_2 ingassing, Fe^{II} and Mn^{II} oxidation, SO_4 reduction, and limestone dissolution, all of which affect pH, are coupled with the same equilibrium speciation and precipitation reactions as the CausticTitrationMix2REYs.exe tool. As explained by Cravotta (2021), a total of 11 treatment steps may be considered, with each having a specified reaction (retention) time, CO_2 outgassing rate ($k_{La,CO2}$); availability of limestone (SAcc.cm2/mol), organic matter (SOC.mol), H_2O_2, sorbent (HMeO.mg), and other variables. A target pH may be specified for the addition of a caustic agent (NaOH, $Ca(OH)_2$, CaO, Na_2CO_3, or $CaCO_3$) to begin steps 1 to 5, possibly after aeration (decarbonation) or other pre-treatment steps. Otherwise, the pH may increase or decrease in response to dynamic, kinetically limited processes. The solution composition at the end of each step is passed to the next step.

2.3   Case study datasets

The PHREEQ-N-AMDTreat+REYs tools were used to simulate AMD treatment and formation of REY-bearing solids, including REYs compounds plus REYs adsorbed onto HFO, HAO, and HMO. Data used for demonstration and corroboration of the PHREEQ-N-AMDTreat+REYs models were obtained from previous studies at passive and active AMD treatment facilities in Pennsylvania (Cravotta and Brady, 2015; Ashby, 2017; Cravotta, 2021). Those studies and others in the Appalachian Coalfield of the eastern USA (Cravotta, 2008; Vass et al., 2019) have identified a wide range of concentrations of REYs in AMD and in solids formed in the treatment of these waters, with generally decreasing REYs concentrations with increasing pH. The models were designed with default values for rate constants, sorbent properties, and mineral precipitation potential to be generally applicable to the range of water-quality conditions in coal AMD and commonly used AMD treatment systems.

3.0   RESULTS AND DISCUSSION

3.1   Field AMD Titration Case Study
The CausticTitrationMix2REYs tool was used to simulate pH and solute concentrations observed during field neutralization of AMD at the Nittany mine (Figs. 1 and 2). The Nittany AMD, which had low pH (3.0) with elevated concentrations of dissolved ($< 0.45 \square$m) Mg (652 mg L^{-1}), Ca (422 mg L^{-1}), Al (128 mg L^{-1}), Mn (129 mg L^{-1}), Fe (40.7 mg L^{-1}), and REYs (2.0 mg L^{-1}), was titrated in the field with 1.6N NaOH to pH 6.0, 7.5, 9.0, and 10.3 (Cravotta et al., 2015; Cravotta and Brady, 2015). Concentrations of dissolved Fe, Al, Mn, and REYs decreased with increased pH; corresponding precipitated solids and sorbent properties were not characterized.

Simulations with the CausticTitrationMix2REYs tool for the Nittanny AMD generally reproduced trends for measured concentrations of Na, Fe, Al, and Mn with increased pH (Fig. 2). Addition of NaOH accounted for increased Na and pH. Decreased concentrations of Fe, Al, and Mn were simulated by the precipitation of solids that formed fresh HFO, HAO, and HMO sorbent. Although simulations assumed equilibrium with $Al(OH)_3$ or basaluminite would limit dissolved Al concentrations, those phases exhibit increased solubility at pH > 8 that is inconsistent with observed low Al concentrations at pH > 8. Formation of a less soluble phase such as kaolinite could possibly explain low Al concentrations; however, kaolinite is not considered by the model.

The simulated REYs concentrations, modeled using default Asp values for HFO, HAO, and HMO, were consistent with empirical trends for REYs attenuation (Fig. 2A). For those conditions, adsorption, mainly by HFO with smaller fractions by HMO, accounts for the decreased REYs concentrations between pH 4 and 8. Adsorption by HAO becomes increasingly important at pH > 7. Precipitation of REYs solids may also attenuate REYs, particularly at pH > 9 (Fig. 2B). Although PO_4 was not detected (< 0.02 mg L^{-1} as P), the PO_4 concentration was assumed to be 0.01 mg L^{-1} in the Nittanny influent. Given that PO_4 concentration, $LaPO_4:10H_2O$ and several other REY-PO_4 phases are supersaturated. As the pH increased to values > 9, $La_2(CO_3)_3$ and some other REY-CO_3 phases also became supersaturated. Simulated precipitation of REYs compounds limited the REYs concentrations to equilibrium with the REYs solids (SI = 0) and, also, decreased the adsorbed fractions over the pH range where the REYs solids could feasibly form (Figs. 2A and 2B).

Fig. 1. User interface (UI) for the CausticTitrationMix2REYs tool showing input values for untreated AMD at the Nittanny mine and adjusted parameters for sorption and precipitation of REYs.

A. Default sorbent Asp values: HFO 600 m² g⁻¹; HAO 68 m² g⁻¹; HMO 746 m² g⁻¹; SI_REY=99
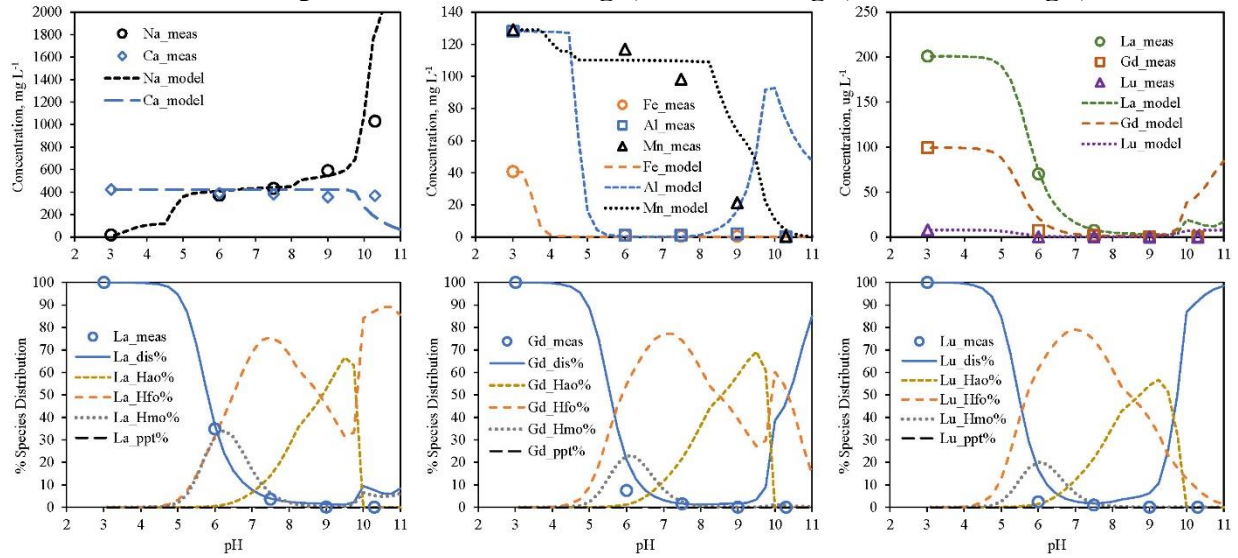
B. Default sorbent Asp values: HFO 600 m² g⁻¹; HAO 68 m² g⁻¹; HMO 746 m² g⁻¹; SI_REY=0
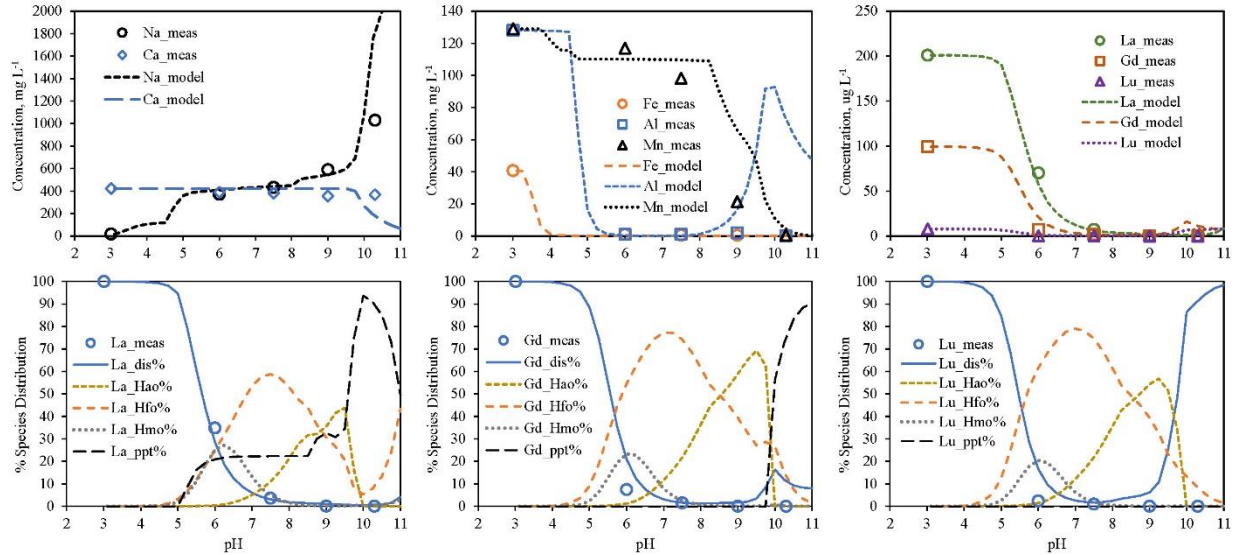
C. Adjusted sorbent Asp values: HFO 700 m² g⁻¹; HAO 774 m² g⁻¹; HMO 850 m² g⁻¹;
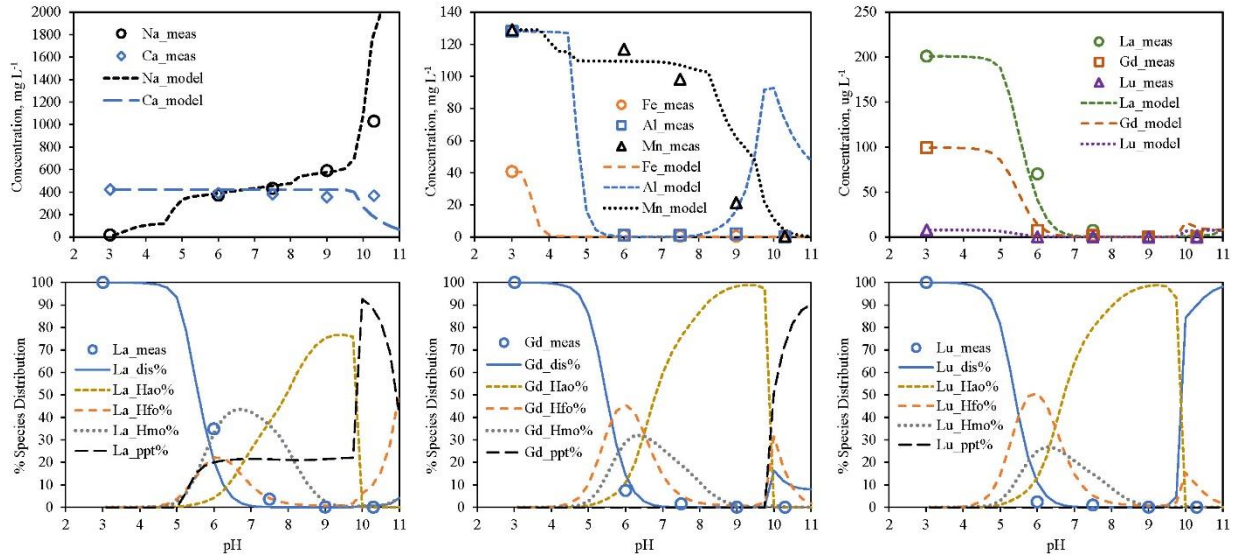
SI$_{REY}$=0

Fig. 2. Results of CausticTitrationMix2REYs model for field titration of Nittanny AMD showing simulation results (curves) compared to measured values (point symbols); measurement errors are roughly the size of symbols. (A) Simulation results for the "fresh" hydrous ferric oxide (HFO), hydrous aluminum oxide (HAO), and hydrous manganese oxide (HMO) sorbent having default values for specific surface area (Asp) and without precipitation of REYs solids; (B) results for same conditions as A *plus* precipitation of REYs; (C) results after increasing Asp to reflect presumed small particle size of the freshly formed sorbent, plus allowing precipitation of REYs.

Alternative fits to observations were obtained by increasing values of Asp for fresh sorbent (Fig. 2C), which may initially precipitate as small particles that have greater Asp than aged, crystalline materials considered for default values. For this scenario, REYs attenuation by all three sorbents is indicated, with HFO predominant at pH ~ 6, HMO at pH ~6.5, and HAO at pH > 7. The modeled Asp of 774 m^2 g^{-1} for HAO, for amorphous Al(OH)$_3$ (Rakotonarivo et al., 1988), is consistent with the Asp used for HFO and HMO. Comparing results shown in the middle and lower sets of graphs (Figs. 2B and 2C) demonstrates that increased Asp causes greater adsorption of La and diminished potential for precipitation of La solids, corresponding to decreased activity of aqueous La^{+3} and decreased saturation index values.

3.2   AMD Treatment Case Studies

To simulate REYs attenuation in a flushable limestone bed, Hedin et al. (2022) applied the CausticTitrationMix2REYs tool with CaCO$_3$ as the titrant and using adjusted Asp values for fresh sorbent. This application of the equilibrium model proved informative, indicating that adsorption on fresh precipitate, alone, could account for observed attenuation of REYs within a limestone bed. However, for complex systems with multiple treatment steps, the TreatTrainMix2REYs model may be appropriate. The TreatTrainMix2REYs sequential model considers the identical equilibrium controls on REYs attenuation in response to variations in pH, solute concentrations, and sorbent properties as the CausticTitrationMix2REYs tool; however, the sequential model simulates disequilibrium conditions with respect to atmospheric exchange, oxidation state of Fe

and Mn, dissolution of limestone (instead of $CaCO_3$ titrant), plus other kinetically limited processes that affect pH, redox state, adsorption, and precipitation.

3.2.1 Pine Forest ALD and Aerobic Wetlands

The TreatTrainMix2REYs tool is used to simulate decreasing aqueous concentrations of REYs within a "biofouled" anoxic limestone drain (ALD) at the Pine Forest passive AMD treatment system, previously described by Cravotta (2021). This treatment system consists of an underground, flushable ALD, oxidation/settling pond, and three aerobic wetlands, in series, with aeration steps in between (Figs. 3 and 4). The untreated AMD (43.5 L s^{-1}), sampled during winter 2015, had pH 5.8 with dissolved oxygen (DO) < 0.5 mg L^{-1} and dissolved concentrations of Fe^{II}, Mn^{II}, and Al of 14.0, 3.1, and 0.09 mg L^{-1}, respectively, and total REYs of 5 mg L^{-1}. The treated effluent had pH ~7, Fe and Mn < 2 mg L^{-1}, and total REYs ~0.6 mg L^{-1}. After its first year of operation (2006), the ALD began to clog with gelatinous, Fe-rich precipitate, which was characterized as biogenic in origin (E. Hince, Geovation Engineering, written commun., 2009). Models simulate Fe and Mn oxidation and the attenuation of REYs with the HMeO precipitate.

For the reported simulations, retention time, CO_2 outgassing rate, available limestone, and pre-existing HMeO mass and composition were varied at each step (Figs. 3 and 4). The fractions of Fe, Al, and Mn in the pre-existing HMeO sorbent were estimated from measured sediment composition at the inflow and points downstream of the ALD (Ashby, 2017). HMeO mass of 75 mg L^{-1} specified for the ALD is consistent with a 0.22-□m thick coating on limestone particles (72 cm^2 mol^{-1}) in contact with 1 L water volume, assuming 35 percent bed porosity and sorbent density of 1.92 g cm^{-3}. For subsequent steps, the specified sorbent mass was only 1 to 3 mg, representing suspended particles and/or coatings on rock or plant surfaces. Consistent values for retention time, $k_{La,CO2}$, and sorbent properties were used for different model scenarios whereby the only values varied were the rate factor for iron-oxidizing bacteria (FeOB) and/or potential for REYs solids to precipitate. For the simulated "biofouling" scenario, the FeOB rate factor (factr.kbact) was increased from 1 to 2; for the abiotic scenario, that factor is 0.

Fig. 3. UI for TreatTrainMix2REYs sequential model showing input values for simulation of water-quality changes through the Pine Forest passive treatment system, December 2015, which consists of a "biofouled" anoxic limestone drain (ALD), oxidation/settling pond, and three aerobic wetlands, with aeration steps in between. The values shown represent enhanced FeOB activity (factr.kbact = 2, instead of default value of 1) and a specified sorbent mass of 85 mg in the ALD with smaller sorbent mass containing progressively greater Mn content downstream. Results of simulations for this scenario and other conditions where values for factr.kbact = 1 or 0 and for REY saturation index = 99 (no precipitation) are shown in Figure 4.

The TreatTrainMix2REYs model results for pH, DO, Fe, Mn, Al, and total REYs at Pine Forest shown as a function of retention time generally reproduce the longitudinal trends for measured constituent values (Fig. 4). The Fe concentration decreased by 30 percent within the ALD, simulated to result from microbial oxidation combined with Fe^{II} sorption and heterogeneous oxidation, leading to the precipitation and accumulation of HFO on limestone surfaces. Simulated attenuation of REYs took place within the ALD because of adsorption by the accumulated HMeO (HFO with lesser quantities of HAO and HMO). Despite less mass of HMeO specified for wetlands downstream of the ALD, greater Mn content of sorbent and increased pH in wetlands (as observed) promoted further attenuation of dissolved Mn^{II} and remaining REYs. Compared to adsorption, REYs precipitation had only a small effect as indicated by the difference between red-dashed (REY precipitation) and blue-dashed curves (no REY precipitation), both simulating the biofouling scenario where the FeOB rate factor was doubled. Simulation results for the two reference scenarios with default (1X) and nullified (0X) FeOB rate factors (Fig. 4, orange solid or black dotted curves) demonstrate that abiotic, Fe^{II} oxidation does not explain observed Fe removal within the ALD but may explain subsequent trends with increased DO and pH. As explained by Cravotta (2021), neutrophilic FeOB are most active under low DO conditions, whereas acidophilic FeOB require low pH.
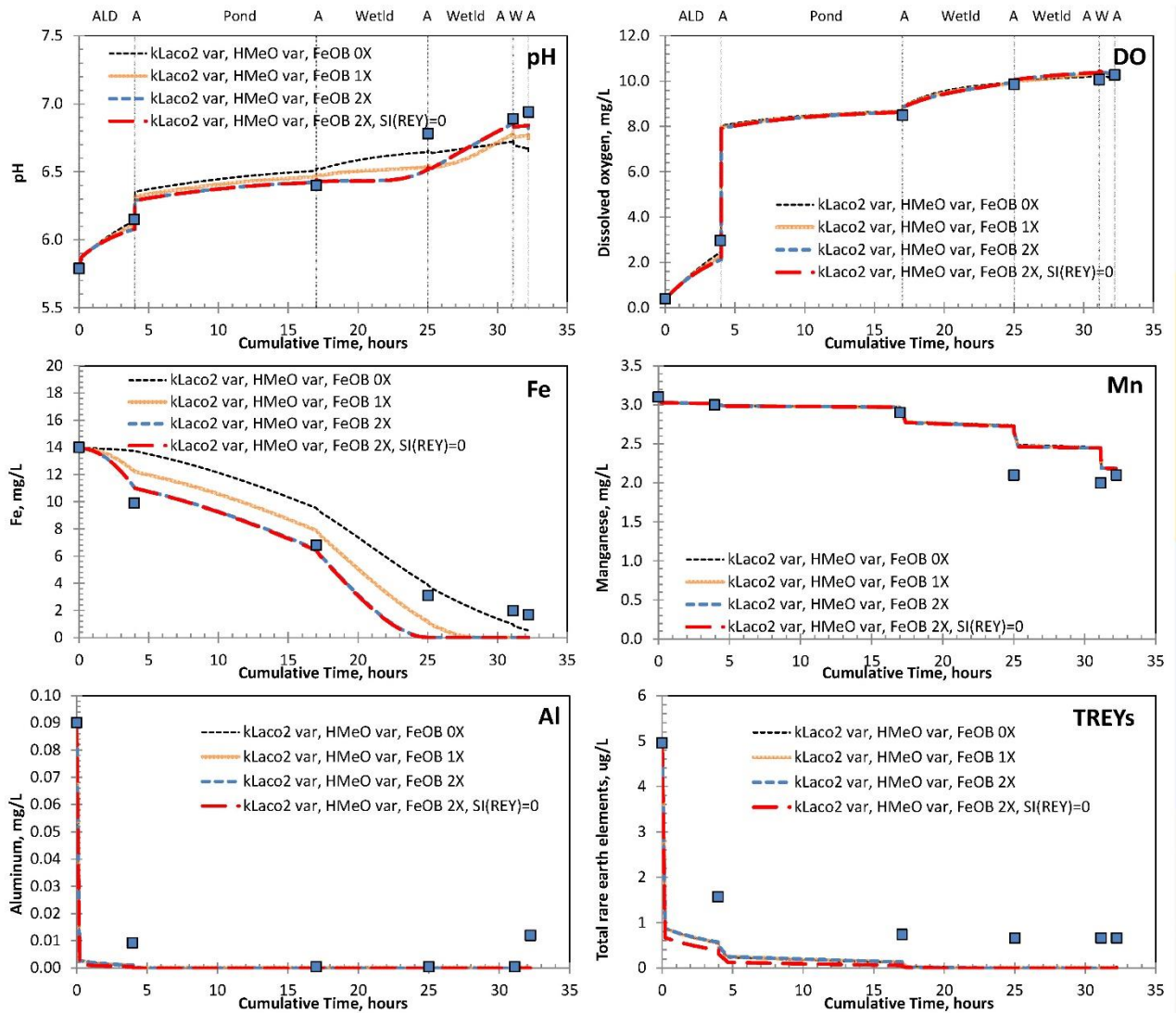
Fig. 4. Comparison of measured (symbols) and simulated (curves) values for pH, Fe, Mn, Al, DO, and total REYs during treatment of AMD at the Pine Forest passive treatment system. Treatment steps are identified at specified times across upper diagrams. Simulations used the TreatTrainMix2REYs sequential model with initial water chemistry for December 2015, specified values for $k_{L,CO2}a$, FeOB rate factor, and sorbent mass and composition (Fig. 3). All models specified sorbent mass in the ALD equivalent to 0.22-□m thick coating on limestone surfaces with smaller sorbent mass having greater Mn content in downstream wetlands. The black dotted curves show results for abiotic conditions (FeOB 0X). The blue or red dashed curves show results for enhanced FeOB activity (FeOB 2X); red curves also simulate REYs minerals precipitation upon reaching saturation (SI(REY)=0).

3.2.2 Silver Creek Aerobic Wetlands

The TreatTrainMix2REYs tool is also used to simulate decreasing aqueous concentrations of REYs within the Silver Creek passive treatment system, described by Cravotta (2021), which

consists of a sedimentation pond, two large oxidation/settling ponds, and two aerobic wetlands, in series, with wide, shallow aeration cascades in between (Figs. 5 and 6). When sampled in 2015 and 2016, the AMD was anoxic with pH 5.9-6.0, concentrations of Fe^{II}, Mn^{II}, and Al of 17.0-20.0, 2.2-2.9, and 0.12-0.17 mg L^{-1}, respectively, and total REYs of 16.5-22.8 mg L^{-1} (Ashby, 2017). Rapid outgassing of CO_2 during aeration steps caused large increases in pH, which facilitated Fe^{II} oxidation in subsequent steps.
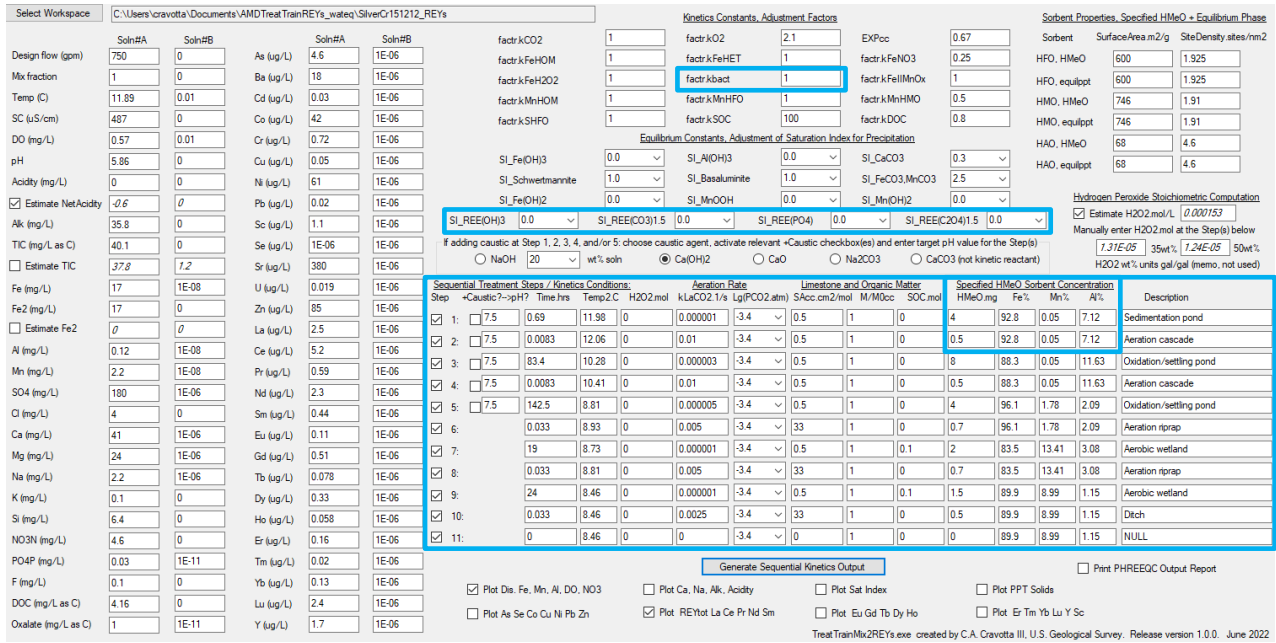

Fig. 5. UI for the TreatTrainMix2REYs sequential model showing input values for simulation of water-quality changes through the Silver Creek treatment system, December 2015, which consists of a small sedimentation pond, two large oxidation/settling ponds, and two aerobic wetlands, with aeration cascades in between. Results of simulations are shown in Fig. 6.

For initial simulations, HMeO composition was based on values reported by Ashby (2017) for sampled sediments at Silver Creek (Fig. 5). The HMeO mass at each step was assumed to be less than or equal to the difference between immediately upstream and downstream samples for the combined mass of Fe, Al, and Mn. Only the CO_2 outgassing rate and sorbent mass and composition (HMeO.mg, Fe%, Mn%, Al%) at each step were adjusted to achieve a reasonable match between empirical and simulated values for longitudinal changes in pH, Fe, Mn, Al, and associated major solute concentrations. Eventual removal of Mn^{II} in the wetland treatment steps were simulated by HMeO sorbent having greater HMO content, as observed for the sampled sediment.

Abiotic oxidation of Fe combined with adsorption and precipitation of solids explains observed attenuation of Fe, Al, Mn, and associated REYs at the Silver Creek treatment system. Microbial Fe oxidation had little effect because of high DO and pH (Fig. 6). Although results for initial simulations effectively reproduced the longitudinal trends for measured pH, DO, Fe, Mn, and Al (Fig. 6, black dashed or orange curves), without REYs mineral precipitation, the corresponding modeled concentrations of total dissolved REYs (and

individual REYs, not shown) remaining in solution were at least five times greater than observed values for all but the last steps of the treatment (Fig. 6, black dashed curves). Simulated precipitation of REYs (SI_REEPO4=0) resulted in a substantial decrease in the concentration of total REYs (Fig. 6, blue or red curves), consistent with observations. Nevertheless, many individual REYs remained undersaturated (e.g. Y, Eu, Gd, Tb, Dy, Ho, Yb, and Lu). As explained by Liu and Byrne (1997), formation of REEPO$_4$ in the environment generally involves co-precipitation of REYs, whereby saturated and undersaturated phases form impure REEPO$_4$ solid solutions.
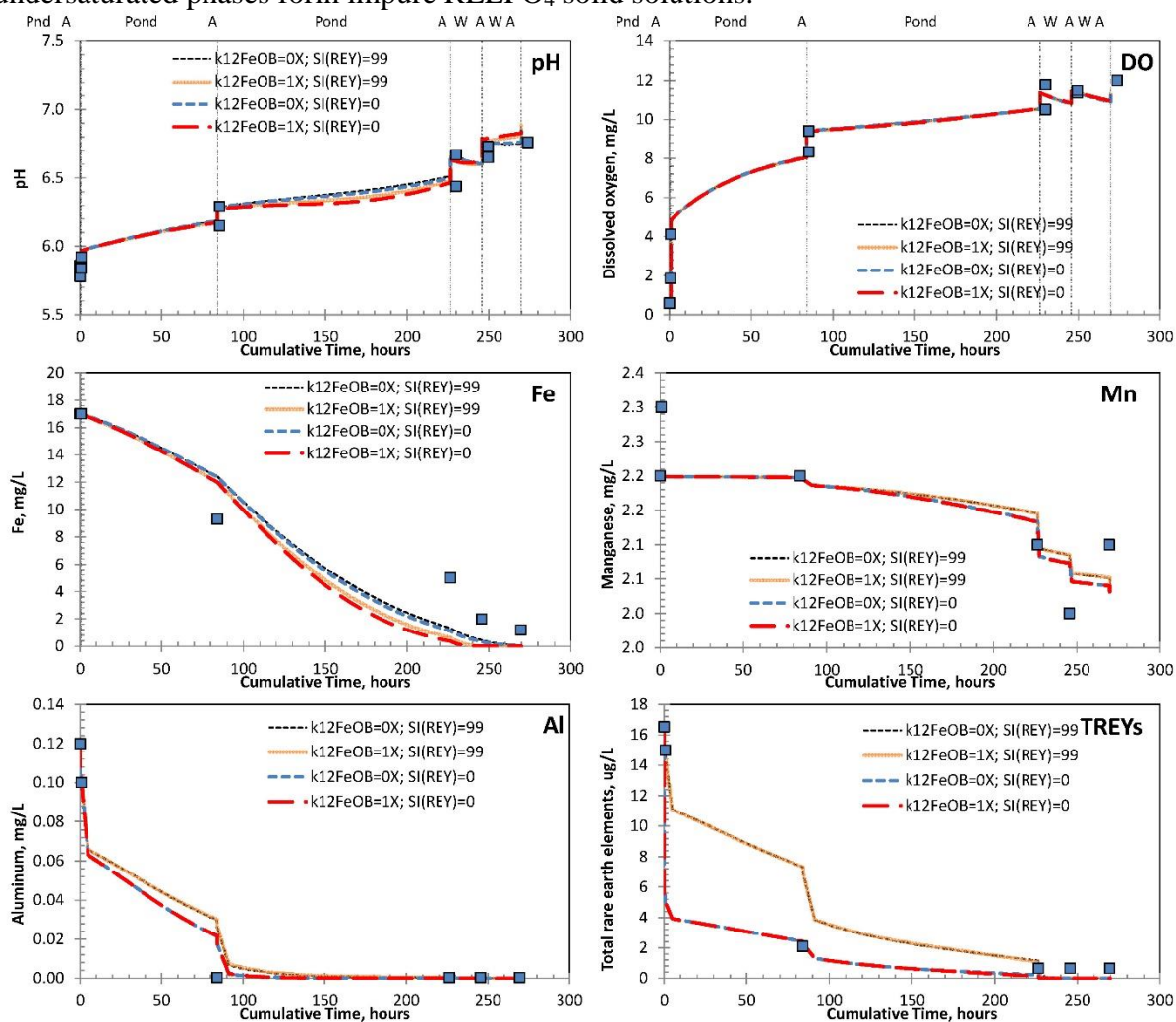
Fig. 6. Comparison of measured (symbols) and simulated (curves) values for pH, DO, Fe, Mn, Al, and total REYs during treatment of AMD at the Silver Creek passive treatment system, December 2015. Treatment steps are identified at specified times across upper diagrams. Simulations used the TreatTrainMix2REYs sequential model with initial water chemistry for December 2015, specified values for k$_{L,CO2}$a, FeOB rate factor, and sorbent mass and composition (Fig. 5). The red dashed curves show results for values in Fig. 5, with specified sorbent having Fe-Mn-Al composition of sediment samples.

3.3 Modeling for Optimization Strategies for REYs Recovery

A goal of modeling with the PHREEQ-N-AMDTreat+REYs tools is to identify strategies that could feasibly produce a concentrated REYs extract from AMD or mine waste leachate that could be valuable. Untreated leachate from a coal-refuse disposal facility in Pennsylvania is considered as a proposed test case for REYs recovery (Figs. 7 and 8). The untreated effluent (9.7 L s^{-1}), sampled during summer 2011, had pH 3.7 with elevated dissolved concentrations of Fe, Mn, and Al of 3,980, 29.75, and 118 mg L^{-1}, respectively, and total REYs of 1,187 mg L^{-1} (Cravotta and Brady, 2015). Current treatment utilizes neutralization with lime, which causes precipitation of Fe, Al, and associated REYs into a complex sludge mixture. If REYs could be concentrated after first removing substantial Fe and Al, the final REYs-bearing phase(s) may be efficiently processed for REYs recovery.

Three treatments to concentrate REYs from the leachate were simulated with the TreatTrainMix2REYs tool. The active lime treatment to pH 8.5 results in nearly complete removal of REYs with Fe-Al-Ca rich sludge (Fig. 8). REYs are diluted by the major metals and other impurities in the sludge. By comparison, alternative treatment strategies using H$_2$O$_2$ to oxidize Fe^{II}, followed by metered addition of Na-caustic agents (NaOH or Na$_2$CO$_3$) to achieve a target pH < 5.5 sequentially remove Fe and Al. Subsequent aeration over an extended time results in the oxidation of Mn which adsorbs and concentrates REYs in the final steps. Alternatively, chemicals such as oxalate or phosphate may be added to the effluent at pH 5.5 to precipitate REYs compounds, following initial steps to remove Fe and Al.

A. Conventional treatment with lime to pH 8.5 and sludge disposal

Select Workspace: C:\Users\Chuck\Documents\AMDTreatTrainREYs_wateq\PBSJob12_REYs

Parameter	Soln#A	Soln#B		Parameter	Soln#A	Soln#B
Design flow (gpm)	153	0		As (ug/L)	275	1E-06
Mix fraction	1.0	0		Ba (ug/L)	6.7	1E-06
Temp (C)	17.95	0.01		Cd (ug/L)	3.4	1E-06
SC (uS/cm)	9740	0		Co (ug/L)	669	1E-06
DO (mg/L)	6.07	0.01		Cr (ug/L)	77.5	1E-06
pH	3.7	0		Cu (ug/L)	19.2	1E-06
Acidity (mg/L)	8335	0		Ni (ug/L)	1029	1E-06
☑ Estimate NetAcidity	10525.6	0		Pb (ug/L)	1.36	1E-06
Alk (mg/L)	0	0		Sc (ug/L)	13	1E-06
TIC (mg/L as C)	23.7	0		Se (ug/L)	8.35	1E-06
☐ Estimate TIC	1.2	1.2		Sr (ug/L)	995	1E-06
Fe (mg/L)	3980	1E-08		U (ug/L)	7.19	1E-06
Fe2 (mg/L)	1000	0		Zn (ug/L)	3850	1E-06
☐ Estimate Fe2	0	0		La (ug/L)	27.2	1E-06
Al (mg/L)	118	1E-08		Ce (ug/L)	115	1E-06
Mn (mg/L)	29.75	1E-08		Pr (ug/L)	22.3	1E-06
SO4 (mg/L)	10500	1E-06		Nd (ug/L)	143	1E-06
Cl (mg/L)	11.7	0		Sm (ug/L)	59.7	1E-06
Ca (mg/L)	411	1E-06		Eu (ug/L)	18.1	1E-06
Mg (mg/L)	303	1E-06		Gd (ug/L)	93.9	1E-06
Na (mg/L)	83.2	1E-06		Tb (ug/L)	17.1	1E-06
K (mg/L)	18.8	0		Dy (ug/L)	95.6	1E-06
Si (mg/L)	25.9	0		Ho (ug/L)	18.5	1E-06
NO3N (mg/L)	0.01	0		Er (ug/L)	48.7	1E-06
PO4P (mg/L)	2.0	1E-11		Tm (ug/L)	6.07	1E-06
F (mg/L)	0.5	0		Yb (ug/L)	35.4	1E-06
DOC (mg/L as C)	0.5	0		Lu (ug/L)	5.29	1E-06
Oxalate (mg/L as C)	0.1	1E-11		Y (ug/L)	481	1E-06

Kinetics Constants, Adjustment Factors

factr.kCO2	1	factr.kO2	2.1	EXPcc	0.67
factr.kFeHOM	1	factr.kFeHET	1	factr.kFeNO3	0.25
factr.kFeH2O2	1	factr.kbact	1	factr.kFeIIMnOx	1
factr.kMnHOM	1	factr.kMnHFO	1	factr.kMnHMO	0.5
factr.kSHFO	1	factr.kSOC	100	factr.kDOC	0.1

Equilibrium Constants, Adjustment of Saturation Index for Precipitation

SI_Fe(OH)3	0.0	SI_Al(OH)3	0.0	SI_CaCO3	2.5
SI_Schwertmannite	1.0	SI_Basaluminite	1.0	SI_FeCO3,MnCO3	2.5
SI_Fe(OH)2	0.0	SI_MnOOH	0.0	SI_Mn(OH)2	0.0
SI_REE(OH)3	0.0	SI_REE(CO3)1.5	0.0	SI_REE(PO4)	0.0	SI_REE(C2O4)1.5	0.0

If adding caustic at Step 1, 2, 3, 4, and/or 5: choose caustic agent, activate relevant +Caustic checkbox(es) and enter target pH value for the Step(s)
○ NaOH 20 wt% soln ○ Ca(OH)2 ◉ CaO ○ Na2CO3 ○ CaCO3 (not kinetic reactant)

Sorbent Properties, Specified HMeO + Equilibrium Phase

Sorbent	SurfaceArea.m2/g	SiteDensity.sites/nm2
HFO, HMeO	600	1.925
HFO, equilppt	600	1.925
HMO, HMeO	746	1.91
HMO, equilppt	746	1.91
HAO, HMeO	68	4.6
HAO, equilppt	68	4.6

Hydrogen Peroxide Stoichiometric Computation
☑ Estimate H2O2.mol/L 0.009135
Manually enter H2O2.mol at the Step(s) below
0.0007723 35wt%, 0.0007314 50wt%
H2O2 wt% units gal/gal (memo, not used)

Sequential Treatment Steps / Kinetics Conditions

Step	+Caustic?->pH?	Time.hrs	Temp2.C	H2O2.mol	k.LaCO2.1/s	Lg(PCO2.atm)	SAcc.cm2/mol	M/M0cc	SOC.mol	HMeO.mg	Fe%	Mn%	Al%	Description
☑ 1:	☐ 7.5	0.033	25	0	0.000001	-3.4	0	1	0	0	0	0	0	Pipe
☑ 2:	☐ 7.5	3.0	25	0	0.000001	-3.4	0	1	0	0	0	0	0	Pond
☑ 3:	☑ 8.5	0.05	25	0	0.00005	-3.4	0	1	0	500	96	1	3	Lime to pH 8.5
☑ 4:	☐ 7.5	0.05	25	0	0.005	-3.4	0	1	0	500	96	1	3	Aeration chambers
☑ 5:	☐ 7.5	20	25	0	0.000001	-3.4	0	1	0	100	96	1	3	Oxidation/settling pond
☑ 6:		0.05	25	0	0	-3.4	0	1	0	0	96	1	3	Injection to mine
☑ 7:		0	25	0	0	-3.4	0	1	0	0	0	0	0	NULL
☑ 8:		0	25	0	0	-3.4	0	1	0	0	0	0	0	NULL
☑ 9:		0	25	0	0	-3.4	0	1	0	0	0	0	0	NULL
☑ 10:		0	25	0	0	-3.4	0	1	0	0	0	0	0	NULL
☑ 11:		0	25	0	0	-3.4	0	1	0	0	0	0	0	NULL

Generate Sequential Kinetics Output   ☐ Print PHREEQC Output Report

☑ Plot Dis. Fe, Mn, Al, DO, NO3   ☐ Plot Ca, Na, Alk, Acidity   ☐ Plot Sat Index   ☐ Plot PPT Solids
☐ Plot As Se Co Cu Ni Pb Zn   ☑ Plot REYtot La Ce Pr Nd Sm   ☐ Plot Eu Gd Tb Dy Ho   ☐ Plot Er Tm Yb Lu Y Sc

TreatTrainMix2REYs.exe created by C.A. Cravotta III, U.S. Geological Survey. Release version 1.0.0. June 2022

B. Alternative treatment with H₂O₂, then NaOH to pH 5.2, aeration steps, and Mn sorption bed

Fig. 7. UI showing the TreatTrainMix2REYs input values for simulation of REYs attenuation from leachate at a coal-refuse disposal facility by conventional and alternative treatment methods.
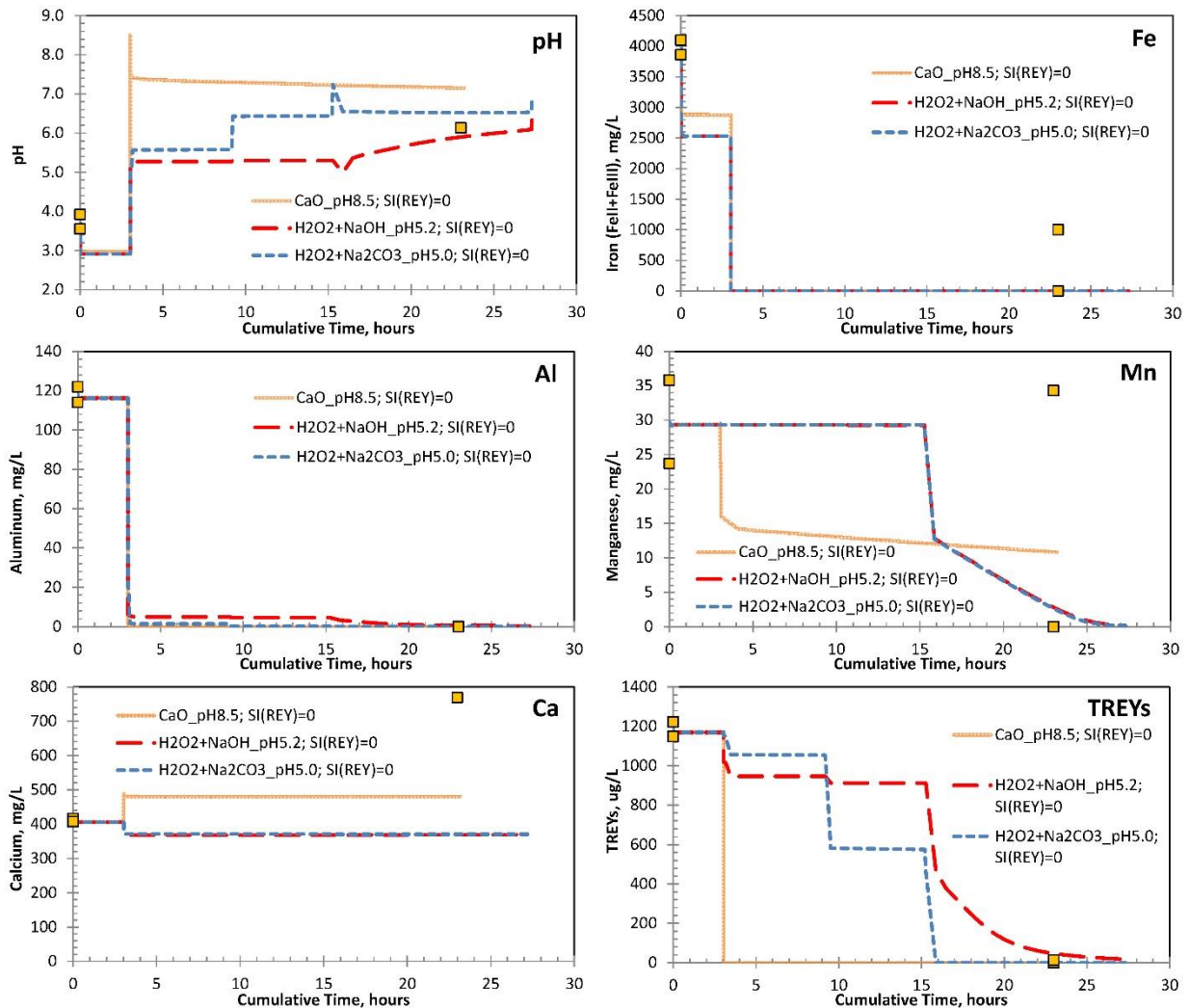
Fig. 8. Comparison of measured (symbols) and TreatTrainMix2REYs simulation results (curves) for pH and dissolved Fe, Al, Mn, Ca, and total REYs concentrations at a coal-refuse disposal facility. Input values for starting water quality and other model variables are shown in Fig. 7. Measured values shown are for lime treatment, sampled on two different dates.

4.0 CONCLUSIONS

The PHREEQ-N-AMDTreat+REYs modeling tools effectively simulate dynamic interactions between Fe, Al, Mn, REYs, and other constituents in complex aqueous systems. Optimization modeling with the TreatTrainMix2REYs tool supports the hypothesis that Fe and Al can be removed from acidic leachate by initial treatment to pH < 5.5 using sequential oxidation and neutralization treatment processes, followed by adsorption and/or precipitation of REYs at higher pH in later steps. The modeling capability of PHREEQC, including aqueous and surface speciation coupled with kinetics of oxidation-reduction and dissolution reactions, provides a quantitative framework for synthesis and application of laboratory equilibrium and rate data to field settings. The UI facilitates adjustment of system variables and the application of the models to evaluate possible design of AMD treatment systems for REYs recovery. Uncertainty in water-quality data, rate data, sorbent quantities and properties, and other system variables can be evaluated by changing values in the UI to identify critical parameters and document

potential variations in results. Field studies that demonstrate REYs attenuation from AMD and corresponding solid-phase formation during specific treatment steps plus laboratory studies of aqueous/solid interactions are helpful to corroborate, refine, and constrain models.

5.0   ACKNOWLEDGMENTS

6.0   REFERENCES

Ashby, E.J., 2017. Biogeochemical mechanisms of rare earth element enrichment in mining-affected aqueous environments. University of Ottawa, Canada, M.S. thesis, 133 p.

Ayora, C., Macías, F., Torres, E., Lozano, A., Carrero, S., Nieto, J.M., Pérez-López, R., Fernández-Martínez, A., and Castillo-Michel, H., 2016, Recovery of rare earth elements and yttrium from passive-remediation systems of acid mine drainage. Environ. Sci. Tech.50, 8255-62.

Ball, J.W., and Nordstrom, D.K., 1991. User's manual for WATEQ4F, with revised thermodynamic data base and test cases for calculating speciation of major, trace, and redox elements in natural waters. U.S. Geol. Surv. Open-File Report 91-183.

Cravotta, C.A. III, 2008. Dissolved metals and associated constituents in abandoned coal-mine discharges, Pennsylvania, USA -- 1. Constituent concentrations and correlations. Appl. Geochem. 23, 166-202.

Cravotta, C.A. III, 2020. Interactive PHREEQ-N-AMDTreat water-quality modeling tools to evaluate performance and design of treatment systems for acid mine drainage (software download). U.S. Geol. Surv. Software Release https://doi.org/10.5066/P9QEE3D5

Cravotta, C.A. III, 2021. Interactive PHREEQ-N-AMDTreat water-quality modeling tools to evaluate performance and design of treatment systems for acid mine drainage. Appl. Geoch., 126, 104845. https://doi.org/10.1016/j.apgeochem.2020.104845.

Cravotta, C.A. III, 2022. Interactive PHREEQ-N-AMDTreat+REYs water-quality modeling tools to evaluate potential attenuation of rare-earth elements and associated dissolved constituents by aqueous-solid equilibrium processes (software download). U.S. Geol. Surv. Software Release https://doi.org/10.5066/P9M5QVK0

Cravotta, C.A. III, and Brady, K.B.C., 2015. Priority pollutants and associated constituents in untreated and treated discharges from coal mines in Pennsylvania, U.S.A.: Appl. Geoch. 62, 108-130.

Cravotta, C.A. III, Means, B., Arthur, W., McKenzie, R., and Parkhurst, D.L., 2015. AMDTreat 5.0+ with PHREEQC titration module to compute caustic chemical quantity, effluent quality, and sludge volume. Mine Wat. Environ. 34, 136-152.

Dzombak, D.A., and Morel, F.M.M., 1990. Surface complexation modeling: Hydrous ferric oxide. John Wiley and Sons, New York, NY, USA.

Edahbi, E., Plante, B., Benzaazoua, M., Ward, M., and Pelletier, M., 2018. Mobility of rare earth elements in mine drainage Influence of iron oxides, carbonates, and phosphates. Chemosphere 199, 647-654.

Fritz, A.G., Tarka, T.J., and Mauter, M.S., 2021. Technoeconomic assessment of a sequential step-leaching process for rare earth element extraction from acid mine drainage precipitates. ACS Sustainable Chemistry and Engineering 9, 9308-9316.

Hedin, B.C., Hedin, R.S., Capo, R.C, and Stewart, B.W., 2020. Critical metal recovery potential of Appalachian acid mine drainage treatment solids. Int. J. Coal Geol. 231, 103610.

Hedin, B.C., Cravotta, C.A. III, Stuckman, M.Y., Lopano, C.L., Capo, R.C, and Hedin, R.S., 2022. Determination and prediction of rare earth element geochemical associations in acid mine drainage treatment wastes. 12th International Conference on Acid Rock Drainage.

Hermassi, M., Granados, M., Valderrama, C., Ayora, C., and Cortina, J.L., 2022. Recovery of rare earth elements from acidic mine waters: An unknown secondary resource. Sci. Tot. Environ. 810, 152258.

Josso, P., Roberts, S., Teagle, D.A.H., Pourret, O., Herrington, R., and Ponce de Leon Albarran, C., 2018. Extraction and separation of rare earth elements from hydrothermal metalliferous sediments. Min. Eng. 118, 106-121.

Karamalidis, A.K., and Dzombak, D.A., 2010. Surface complexation modeling: Gibbsite. John Wiley & Sons, Inc., Hoboken, NJ, USA.

Leon, R., Macias, F., Canovas, C.R., Perez-Lopez, R., Ayora, C., Nieto, J.M., and Olias, M., 2021. Mine waters as a secondary source of rare earth elements worldwide: The case of the Iberian Pyrite Belt. J. Geoch. Explor. 224, 106742.

Liu, X., and Byrne, R.H., 1997. Rare earth and yttrium phosphate solubilities in aqueous solution. Geochim. Cosmochim. Acta 61, 1625-1633.

Liu, H., Pourret, O., Guo, H., and Bonhoure, J., 2017. Rare earth elements sorption to iron oxyhydroxide: Model development and application to groundwater. Appl. Geoch. 87, 158-166.

Lozano, A., Ayora, C., and Fernández-Martínez, A., 2019. Sorption of rare earth elements onto basaluminite: The role of sulfate and pH. Geochim. Cosmochim. Acta 258, 50-62.

Mwewa, B., Tadie, M., Ndlovu, S., Simate, G.S., and Mitinde, E., 2022. Recovery of rare earth elements from acid mine drainage: A review of the extraction methods. J. Environ. Chem. Eng. 10, 107704.

Office of Surface Mining Reclamation and Enforcement, 2017. AMDTreat. https://amd.osmre.gov/

Parkhurst, D.L., and Appelo, C.A.J., 2013. Description of input and examples for PHREEQC version 3—A computer program for speciation, batch-reaction, one-dimensional transport, and inverse geochemical calculations. U.S. Geol. Surv. Techniques Methods 6-A43.

Pourret, O., and Davranche, M., 2013. Rare earth element sorption onto hydrous manganese oxide: a modeling study. J. Colloid Interface Sci. 395, 18-23).

Rakotonarivo, E., Bottero, J.Y., Thomas, F., Poirier, J.E., and Cases, J.M., 1988. Electrochemical modeling of freshly precipitated aluminum hydroxide-electrolyte interface. Colloids and Surfaces 33, 199-207.

Royer-Lavallée, A., Neculita, C.M., and Coudert, L., 2020. Removal and potential recovery of rare earth elements from mine water. J. Indust. Chem. Eng. 89, 47-57.

Tonkin, J.W., Balistrieri, L.S., and Murray, J.W., 2004. Modeling sorption of divalent metal cations on hydrous manganese oxide using the diffuse double layer model. Appl. Geoch., 19, 29-53.

Vass, C.R., Noble, A., and Ziekiewicz, P., 2019. The occurrence and concentration of rare earth elements in acid mine drainage and treatment byproducts. Part 2: regional survey of northern and central Appalachian coal basins. Mining Metal. Explor. 36, 917-929.

Verplanck, P.L., Nordstrom, D.K., Taylor, H.E., and Kimball, B.A., 2004. Rare earth element partitioning between hydrous ferric oxides and acid mine water during iron oxidation. Appl. Geoch. 19, 1339-1354.

Wang, Y., Ziemkiewicz, P., and Noble, A., 2021. A hybrid experimental and theoretical approach to optimize recovery of rare earth elements from acid mine drainage precipitates by oxalic acid precipitation. Minerals 12, 236.

Zhang, W., and Honaker, R.Q., 2018. Rare earth elements recovery using staged precipitation from a leachate generated from coarse coal refuse. Int. J. Coal Geol. 195, 189-199.